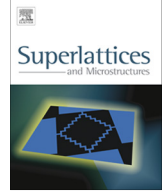




ELSEVIER

Contents lists available at ScienceDirect

Superlattices and Microstructures

journal homepage: www.elsevier.com/locate/superlattices

A novel thermo-photovoltaic cell with quantum-well for high open circuit voltage



Ezzat Sadat Kouhsari ^{a,*}, Rahim Faez ^b, Maedeh Akbari Eshkalak ^c

^a Department of Electro Technique, College of Electrical Engineering, Yadegar-e-Imam Khomeini (Rey) Shahre-rey Branch, Islamic Azad University, Tehran, Iran

^b Department of Electrical Engineering, Sharif University of Technology, Tehran, Iran

^c Department of Electrical Engineering, Karaj Branch, Islamic Azad University, Karaj, Iran

ARTICLE INFO

Article history:

Received 27 December 2014

Received in revised form 6 March 2015

Accepted 10 March 2015

Available online 17 March 2015

Keywords:

Thermo photovoltaic cell

Tandem cells

Solar cells with quantum-wells

ABSTRACT

We design a thermo-photovoltaic Tandem cell which produces high open circuit voltage (V_{oc}) that causes to increase efficiency (η). The currently used materials (AlAsSb–InGaSb/InAsSb) have thermo-photovoltaic (TPV) property which can be a p – n junction of a solar cell, but they have low bandgap energy which is the reason for lower open circuit voltage. In this paper, in the bottom cell of the Tandem, there is 30 quantum wells which increase absorption coefficients and quantum efficiency (QE) that causes to increase current. By increasing the current of the bottom cell, the top cell thickness must be increased because the top cell and the bottom cell should have the same current. In the top cell, by increasing the thickness, absorption coefficients and quantum efficiency increase that causes to increase the current. Current increment is also the second factor that causes to increase overall efficiency.

© 2015 Elsevier Ltd. All rights reserved.

1. Introduction

In the quest for renewable energy sources, mankind has placed great interest and re-sources toward the progression of photovoltaic. As this interest has grown, various types of solar cells have

* Corresponding author. Tel.: +98 919 259 2854.

E-mail address: eskoohsari467@gmail.com (E.S. Kouhsari).

been produced: organic, thin films II–IV, single crystalline silicon, single-junction III–V, Tandem and multi-junction (MJ) III–V cells [1].

Using Tandem solar cells is one of the methods to achieve high efficiency in transforming solar energy into electricity. These solar cells made of III–V semiconductors can be arranged in a cascade architecture which increases their efficiency. A tunnel diode structure is thus normally used. The optical and electrical losses of these diodes must be as low as possible in order not to affect the increased efficiency of the cells. A small thickness of cascaded layers and large rates of I_p/V_p can lower the optical and electrical losses, respectively. On the other hand, in the process of tunnel diode production, high density of dopants will result in crystal defects and light absorption. Also unwanted diffusion of impurity atoms may occur when subsequent layers are grown [2].

In multi-junction solar cells such as Tandem, each cell converts a portion of the solar spectrum into electrical energy that causes the optimized use of the spectrum [3].

Tandem is made when the junctions are stacked on top of one another in series, the cells can be modeled as an equivalent series circuit such that the output current would be limited by the junction to produce the least amount of current. So, to increase the least amount of the current, a technology such as QWs can be used. On the other hand, the voltages of each junction must add to each other [1].

The trade-off between incorporation of a sufficient number of quantum wells ensures high photon absorption efficiency and increased short-circuit current. That is, extending of absorption spectrum leads to longer wavelengths [4].

The rate of radiative emission from the QWs can be calculated from the knowledge of the absorption coefficient and applying the principle of detailed balance [5].

Thermo-photovoltaic (TPV) systems are subsequently converted into electron-hole pairs via a low-bandgap photovoltaic (PV) medium; these electron-hole pairs are then conducted to the leads to produce a density current [6]. The obvious difference between solar photovoltaics and thermo photovoltaics is that a TPV system generates its own light. As a result, high efficiency is possible by tailoring the emission spectrum to match the spectral response (or quantum efficiency) of the TPV cells [7].

III–V group semiconductors are suitable for TPV cells since their narrow direct band-gaps in a range from 0.3 eV to 0.7 eV closely match to the peak wavelength of the thermal source [8].

Electrode			
Window	AlAsSb	N	} Top cell
Emitter	AlAsSb	N	
Base	InGaSb	P	
BSF	AlAsSb	P	
Buffer	AlAsSb	P	
Tunnel Junction	InGaSb	P ⁺	} Tunnel Junction
Tunnel Junction	InGaSb	N ⁺	
Window	InGaSb	N	} Bottom cell
Emitter	InAsSb	N	
25 stack QWs	InGaSb/ InAsSb		
Base	InAsSb	P	
BSF	InGaSb	P	
Buffer	InGaSb	P	
Electrode			

Fig. 1. A double junction AlAsSb–InGaSb/InAsSb Tandem solar cell.

Table 1

Characteristics of the first cell.

	Window	Emitter	Base	BSF	Buffer
Material	AlAsSb	InGaSb	InGaSb	AlAsSb	InGaSb
Thickness (μm)	0.015625	0.026	0.05	0.003125	0.009375
Doping (cm^{-3})	5e19	4.64e17	1e17	5e19	1e18

Table 2

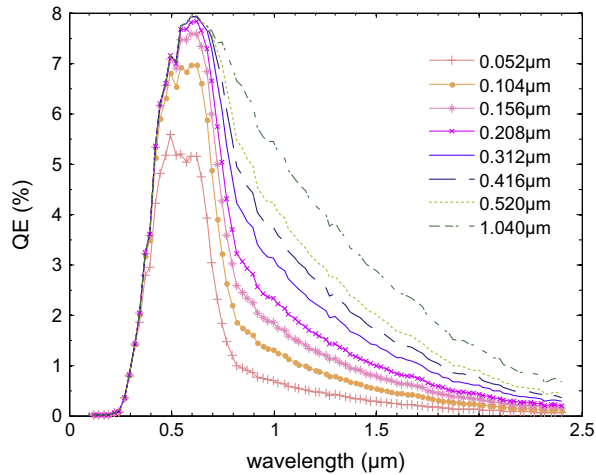
Characteristics of the second cell.

	Window	Emitter	Base	BSF	Buffer
Material	InGaSb	InAsSb	InAsSb	InGaSb	InAsSb
Thickness (μm)	0.01	0.01	0.44	0.2	0.3
Doping (cm^{-3})	4.64e17	4.64e15	1e17	5e19	7e18

Table 3

Parameters of material.

Material	X	Y	E_g	Affinity	Permittivity
AlAsSb	–	0.042	1.69	3.6105	11.957
InGaSb	0.923	–	0.675	4.1	15.845
InAsSb	–	0.857	0.32	4.856	15.8146

**Fig. 2.** EQE characteristics of a top cell with various thickness.

Many III–V group semiconductors, such as InGaSb, InAsSb and AlAsSb have been investigated for TPV applications [9–12].

In this paper, monolithically stacked AlAsSb/InGaSb–InAsSb Tandem TPV cell with MQW is designed and simulated. The characteristics of the AlAsSb/InGaSb–InAsSb Tandem TPV cells, including absorption coefficients and quantum efficiency I – V curve, P_{max} , V_{oc} , and J_{sc} , are analyzed. We try to increase open circuit voltage along with proportional suitable short circuit current. So, we design a two junction photovoltaic cell with quantum well composed of InGaSb, AlAsSb and InAsSb and stimulate it by Silvaco software. Current–voltage curves and quantum power–efficiency are studied. At last, this cell will be compared with three traditional Tandem thermo-photovoltaic cells.

2. Cell structure

Fig. 1 illustrates the structure of a Tandem AlAsSb–InGaSb/InAsSb solar cell, that consists of a AlAsSb–InGaSb $p-n$ heterojunction as the top cell, and a InAsSb $p-n$ homojunction as the bottom cell. The dimension, material types and doping characteristics of the top cell and the bottom cell are shown in Tables 1 and 2. The InGaSb tunnel junction with a 30 nm thickness and a heavily doped provides electrical connection between top and bottom cells. However, in the thermal process of InGaSb cell production, current–voltage behavior of this tunnel diode becomes more non-ideal and current peak decreases [2].

Photon coupling between subcells in a Tandem device has been studied in the past [5]. However, a multi quantum well (MQW) bottom cell can be expected to make photon coupling more significant than that of the conventional bulk devices. The top cell emitter, base, and tunnel junctions are transparent to the photons that are radiated, leading to less parasitic absorption; so, a greater fraction of photons being absorbed by the bottom cell.

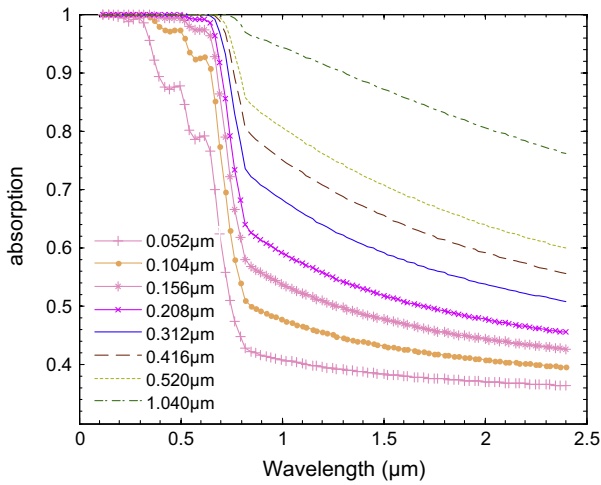


Fig. 3. Spectral directional absorptivity (emissivity) of a top cell by various thickness.

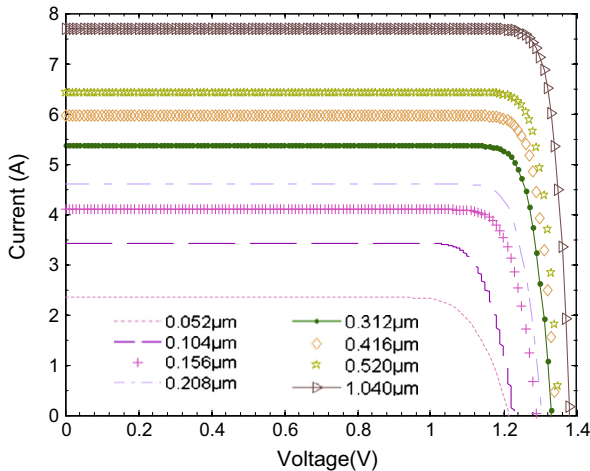


Fig. 4. $I-V$ curves of a top cell by various thicknesses.

As a result, photon coupling needs to be taken into account when predicting the performance of MQW Tandem solar cells. In other hands, subcells should be matching current. In order to achieve a suitable current in second cell, twenty five wells made of InAsSb with thickness of 11.7 nm and twenty five barriers made of InGaSb with thickness of 41.5 nm are applied.

In this paper, we used materials that have crystal lattice matching. The place of these materials is 6.12 Å which is seldom used. The characteristics of these materials used in this cell are listed in Table 3.

3. Models

In this paper, thermo-photovoltaic cell is designed and simulated by Atlas simulator from the Silvaco software. When a sufficiently high electric field exists within a *p-n* junction, local bands may bend sufficiently to allow electrons to tunnel, by the means of internal field emission, from the

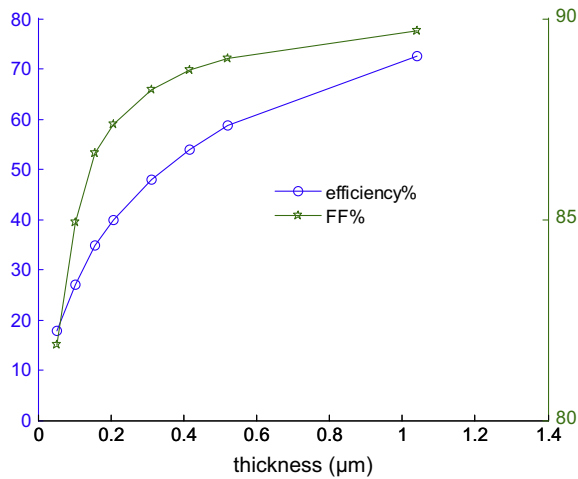


Fig. 5. FF and efficiency of a top cell by various thickness.

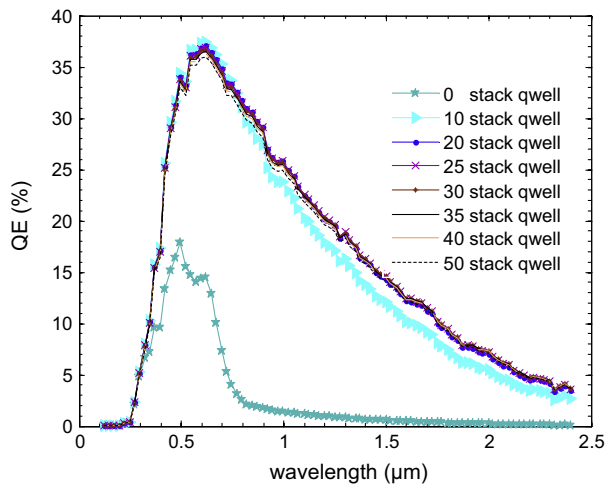


Fig. 6. QE characteristics of a bottom cell with different numbers of QWs.

valence band into the conduction band; Meanwhile, a symmetric behavior occurs for the holes. An additional electron, therefore, transfers to the conduction band, and a hole transfers to the valence band. Local band-to-band tunnelling models can be employed to reproduce the behavior of such devices. These models, when implemented inside a technology computer-aided design (TCAD) environment, use the electric field value at each node along the junction to give a generation rate at that point due to tunnelling. In reality, the tunnelling process is nonlocal, and it is necessary to account for the spatial profile of the energy bands. The model assumes that the tunnelling is 1-D in nature; so, it can be calculated by using a special rectangular mesh of nanometer size superimposed over and coupled to the ATLAS regular mesh [13]. SRH, Auger and surface recombinations are chosen for the carrier recombination models [14]. We can enable the quantum well model by specifying QWELL in the REGION or MODELS statement. The orientation and dimensionality of Schrodinger solver is set by SP.GEOMETRY parameter on the MODELS statement with a default of 1DY. Alternatively,

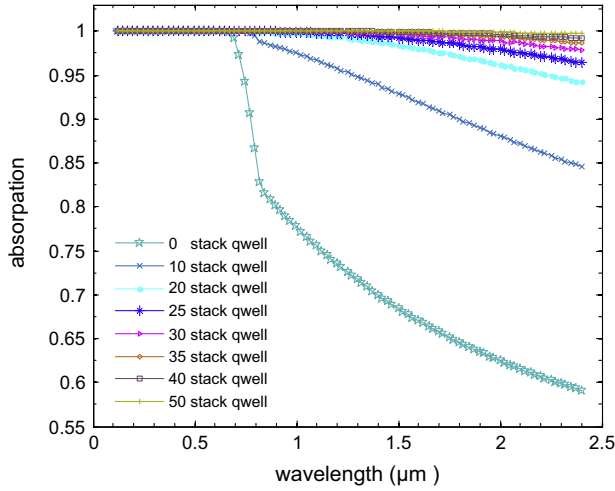


Fig. 7. Spectral directional absorptivity (emissivity) of a bottom cell with different numbers of QWs.

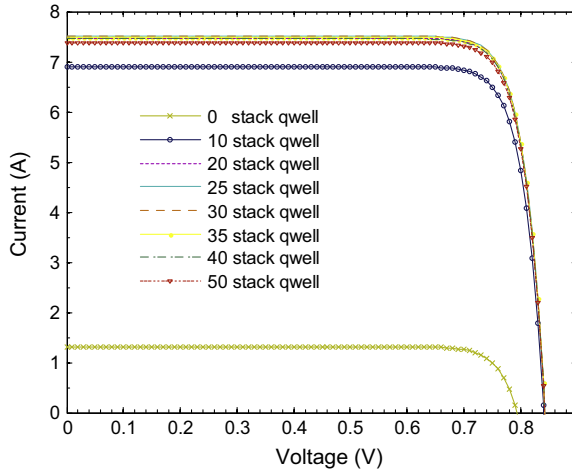


Fig. 8. I–V curves of a bottom cell with different numbers of QWs.

we may solve 1DX and 1DZ cases [14]. In simulating of thermo-photovoltaic cell, blackbody spectrum of 5800 K is applied. In special application, this spectrum, along with environment temperature, will change.

V_{oc} , I_{sc} , FF, η and quantum efficiency are important index for a solar cell. Atlas simulator calculates V_{oc} and I_{sc} of $p-n$ junction, but the fill factor (FF) and power conversion efficiency (η) were calculated by using equations below. The fill factor, FF is the ratio of maximum power point (P_m) divided by the I_{sc} and V_{oc} , and that is:

$$FF = \frac{I_m V_m}{I_{sc} V_{oc}} = \frac{P_m}{I_{sc} V_{oc}} \tag{1}$$

The energy conversion efficiency of solar cell, η is the comparison of maximum power point of cell, P_m to input light from source, P_{in} , [15]

$$\eta = \frac{P_m}{P_{in}} \times 100\% = \frac{FF \cdot I_{sc} \cdot V_{oc}}{P_{in}} \times 100\% \tag{2}$$

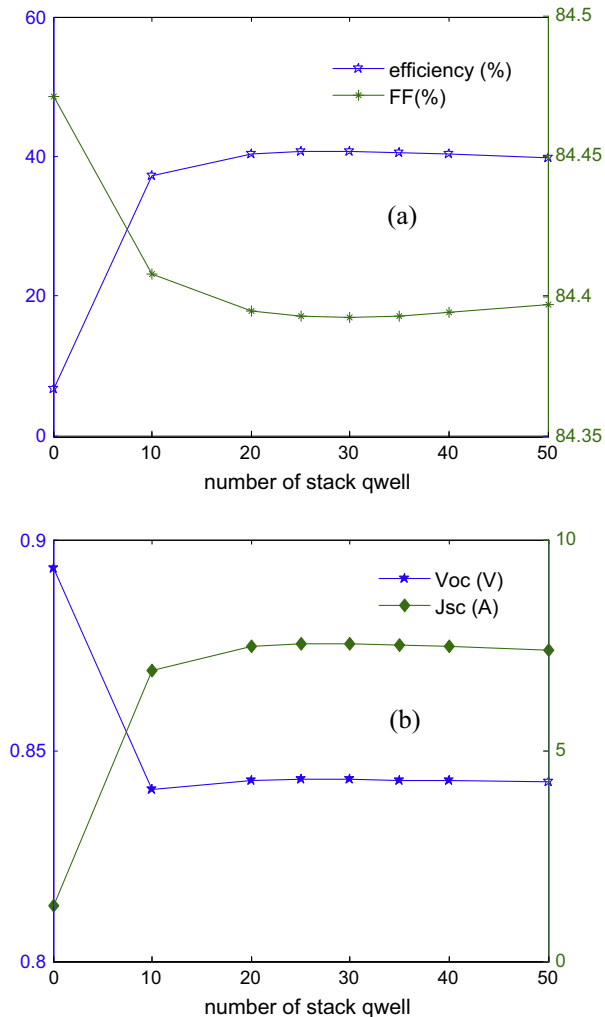


Fig. 9. (a) V_{oc} and I_{sc} , (b) FF and efficiency of a top cell with various thicknesses.

4. Simulation results

We derived absorption coefficients, quantum efficiency, I - V and variety of V_{oc} , I_{sc} , FF via the thickness in top cell and via number of MQW in the bottom cell [16]. Finally, we select suitable thickness for top cell and suitable number of MQW for bottom cell because these cells must have current matching for optimization of result.

Junction thickness is a critical design parameter for single-junction solar cells. To make the discussion more general and more useful for practical devices, the effective absorption (i.e., the “optical thickness” of a solar cell junction), which is strongly material dependent is investigated, rather than the physical thickness of the junction. Using a AlGaSb–InGaSb single-junction solar cell with different thicknesses, we have plotted the energy quantum efficiency via the effective absorption for the black-body 5600 K solar spectrum as shown in Fig. 2.

In first step, we focus only on the optical properties of our cells, i.e., on the quantum efficiency and absorption coefficient. By increasing the thickness of the cell, according to Fig. 2, wide spectrum is increased and according to Fig. 3, the wide spectrum photons can be absorbed efficiently.

According to Figs. 4 and 5 V_{oc} , I_{sc} , η and FF are increased by increasing the absorption coefficient and quantum efficiency. Increasing of these parameters is not linear.

InAsSb is used for the bottom cell. The quantum efficiency and absorption coefficient are shown in Figs. 6 and 7. This cell has a little I_{sc} . We want to increase I_{sc} . So, we should use the QWs. According to Figs. 6 and 7, with increasing number of stack QWs, quantum efficiency and absorption coefficient are increasing, until the number of the stacks be 25. Quantum efficiency is almost constant and absorption coefficient is a little various for 25,30,35 and 40 stacks.

The I - V curves for the bottom cell with different numbers of QWs are plotted in Fig. 8. I_{sc} , V_{oc} , η and FF with different numbers of QWs are plotted in Fig. 9. These figures show I_{sc} and to increase and V_{oc} and FF to decrease.

I_{sc} and η are not big various between 20 and 35 QWs stack. Maximum I_{sc} and η is calculated for 25 QWs stack.

When the top cell is stacked on the bottom cell in series, if the top junction in a Tandem solar cell generates more current than the limiting current in the other subcells, the extra current will be redistributed to increase the limiting current in the lower subcells. This is achieved by thinning the top junction to allow some of the spectrum to get absorbed, instead, in the lower cells. This redistribution of the solar spectrum between the subcells results in a higher limiting current. According to Fig. 10, If the top cell has more thickness, this cell will absorb more spectrum; so, the bottom cell gets the remaining solar spectrum and generates less current. It causes to generate less current as shown in

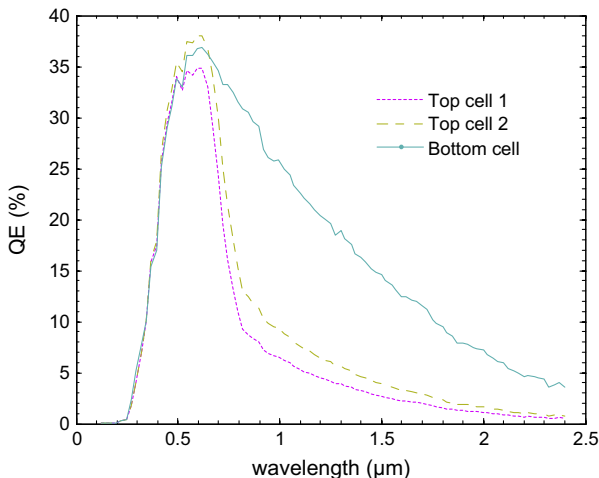


Fig. 10. QE characteristics of a Tandem with two thickness of the top cell.

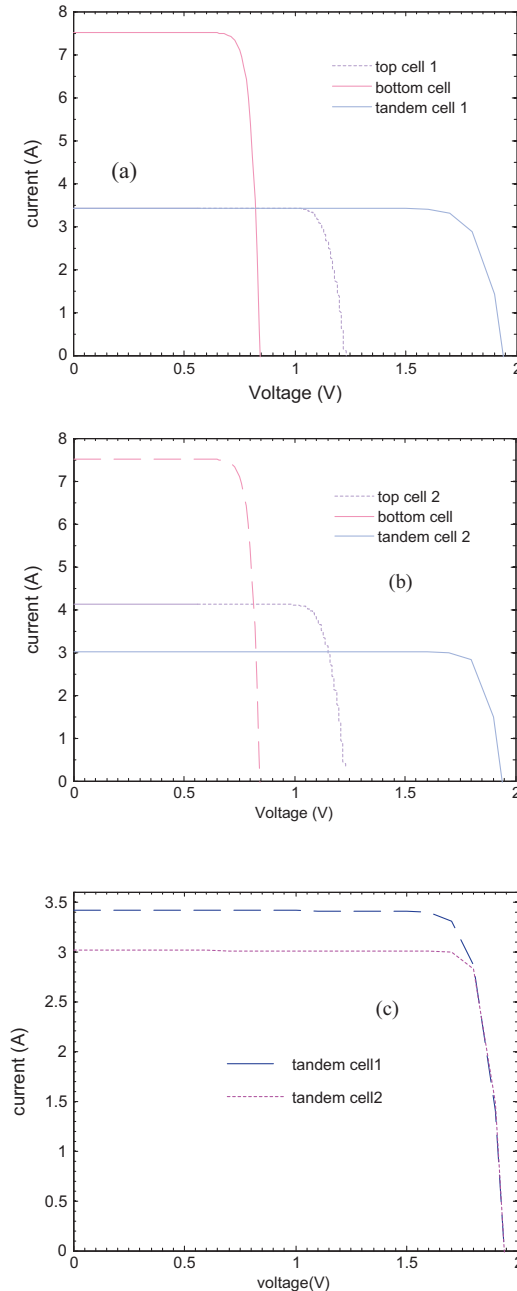


Fig. 11. (a) *I-V* curve of the Tandem1 with 0.104 μm thickness of top cell1, (b) *I-V* curve of the Tandem2 with 0.156 μm thicknesses of top cell2, (c) *I-V* curve of two Tandems with different top cell thicknesses.

Fig. 11, because the top and bottom cells should have matching current. In other hands, the top cell should generate a current, then the bottom cell will also generate the same current with the remaining solar spectrum that it can absorbed. In **Fig. 11(a)**, the top cell has 0.104 μm and generates 3.42 A and as a result, the Tandem cell has 3.42 A current. In **Fig. 11(b)**, the top cell has 0.156 μm and generates 4.2 A

and Tandem cell has 3 A. This different current is shown in Fig. 11(c). V_{oc} in both of the cells is constant and efficiency is increased.

The Tandem TPV cells are simulated with the optimized parameters listed in Tables 2 and 3. The TPV cell area (W_{cell}) is $500 \mu\text{m} \times 500 \mu\text{m}$. The radiation temperature (T_{rad}) is 5600 K, with the cell temperature (T_{cell}) of 300 K Fig. 11(b) shows the I - V curves of the Tandem cells and of the single-cells. Comparing with the seldom reported GaSb–GaInAsSb Tandem TPV cells in Refs. [8,17 and 18], which acquire a maximal V_{oc} of 1.8 V; the V_{oc} of the InGaSb–InAsSb Tandem TPV cells we simulated is as high as 1.8 V. It proves that the structure of our Tandem TPV cell is more advanced. The result shows that P_s of the Tandem cells is more than those of the InGaSb and the InAsSb cells.

5. Conclusion

A new structure is proposed for the Tandem thermo-photovoltaic solar cells that has more V_{oc} and efficiency.

The current, voltage, efficiency, and FF versus quantum efficiency and absorption coefficient for three solar cell structures have been investigated by using the two-dimensional numerical photovoltaic cell simulator Silvaco/Atlas. The Tandem TPV cells consist of a InGaSb heterojunction as the top cell and a InAsSb homojunction as the bottom cell. Matching current between the top cell and bottom cell is very important and current of each cell depends on the structure of the cells.

For further improvements of the Tandem cell performance, in order to increase the collection efficiency of the photon-generated carriers, the Tandem cell is converted to three junction solar cell by quantum dot technology.

References

- [1] Seth M. Hubbard, John D. Andersen, Modeling concentrator solar cells using detailed balance and numerical approaches, Timothy Bald (2012).
- [2] J. Fariborz, S. Mirzakhchaki, A new structure in Tandem solar cells, *Int. J. Mod. Eng. Res. (IJMER)* 2 (6) (2012) 4014–4018. ISSN: 2249-6645.
- [3] Nikhil Jain, Design of V multijunction solar cells on silicon substrate, Master of Science in Electrical Engineering, Blacksburg, VA[5], 2013.
- [4] D. Derkacs, W.V. Chen, P.M. Matheu, S.H. Lim, P.K.L. Yu, E.T. Yu, Nanoparticle-induced light scattering for improved performance of quantum-well solar cells, *Appl. Phys. Lett.* 93 (2008) 091107.
- [5] Kan-Hua Lee, Keith W.J. Barnham, James P. Connolly, Benjamin C. Browne, Robert J. Airey, John S. Roberts, Markus Fuhrer, Thomas N.D. Tibbits, Nicholas J. Ekins-Daukes, Demonstration of photon coupling in dualmultiple-quantum-well solar cells, *IEEE J. Photovoltaics* 2 (1) (2012).
- [6] Peter Bermel, Michael Ghebrebrhan, Walker Chan, Yi Xiang Yeng, Mohammad Araghchini, Rafif Hamam, Christopher H. Marton, Klavs F. Jensen, Marin Soljacić, John D. Joannopoulos, Steven G. Johnson, Ivan Celanovic, Design global optimization of high-efficiency thermo photovoltaic systems, *Opt. Expr. OSA* 18 (103) (2010) A314–A334.
- [7] Walker Chan, Towards a High-Efficiency Micro-Thermo Photovoltaic Generator, Master of Engineering in Electrical Engineering at the Massachusetts Institute of Technology, 2010.
- [8] Yang Hao-Yu, Liu Ren-Jun, Wang Lian-Kai, Lu You, Li Tian-Tian, Li Guo-Xing, Zhang Yuan-Tao, Zhang Bao-Lin, The design and numerical analysis of Tandem thermo photovoltaic cells, *Chin. Phys. B* 22 (10) (2013) 108402, <http://dx.doi.org/10.1088/1674-1056/22/10/108402>.
- [9] Oleg V. Sulima, A.W. Bett, P.S. Dutta, M.G. Mauk, GaSb-, InGaAsSb-, InGaSb-, InAsSbP- and Ge-TPV cells with diffused emitters, *IEEE Phot. Spec. Conf.* (2002) 892–895, <http://dx.doi.org/10.1109/PVSC.2002.1190723>.
- [10] M. Zierak, J.M. Borrego, I. Bhat, R.J. Gutmann, G. Charache, Modeling of InGaSb Thermo photovoltaic cells and materials, in: 3. NREL Conference on Thermo Photovoltaic (TPV) Generation of Electricity, Colorado Springs, 1997, <http://dx.doi.org/10.2172/319651>, <http://www.researchgate.net/publication/234997916_Modeling_of_InGaSb_thermophotovoltaic_cells_and_materials>.
- [11] Jian Yin, Roberto Paiella, Multiple-junction quantum cascade photodetectors for Thermo photovoltaic energy conversion, *Opt. Expr. OSA (C)* 18 (2) (2010).
- [12] E. Jamie, Van Dyke, Modeling Laser Effects on Multi-Junction Solar Cells Using Silvaco Atlas Software for Spacecraft Power Beaming Applications, Master of Science in Space Systems Operations from the Naval Postgraduate School, 2010.
- [13] Mathieu Baudrit, Carlos Algora, Senior Member, Tunnel diode modeling including nonlocal trap-assisted tunnelling: a focus on III-V multi-junction solar cell simulation, *IEEE Trans. Electr. Dev.* 57 (10) (2010).
- [14] ATLAS User's Manual, Silvaco International 2, 2010.
- [15] Lennie, H. Abdullah, S.M. Mustaza, K. Sopian, Photovoltaic properties of Si_3N_4 layer on silicon solar cell using Silvaco Software, *Eur. J. Sci. Res.* 29 (4) (2009). ISSN 1450-216X.
- [16] Thomas Kirchartz, Kaori Seino, Jan-Martin Wagner, Uwe Rau, Friedhelm Bechstedt, Efficiency limits of Si/SiO₂ quantum well solar cells from first-principles calculations, *J. Appl. Phys.* 105 (2009) 104511.
- [17] M.G. Mauk, V.M. Andreev, *Semicond. Sci. Technol.* 18 (2003) S191.
- [18] V.M. Andreev, V.P. Khvostikov, V.D. Rumyantsev, S.V. Sorokina, M.Z. Shvarts 2000 Proceedings of the 28th IEEE Photovoltaic Specialists Conference, Anchorage, USA, September 15–22, 2000, p. 1265.